

Longitudinal-Transverse Interference Structure Function of ${}^2\text{H}$

M. van der Schaar,^{(1),(2)} H. Arenhövel,⁽³⁾ H. P. Blok,^{(2),(4)} H. J. Bulten,⁽²⁾ E. Hummel,⁽⁵⁾ E. Jans,⁽²⁾ L. Lapidás,⁽²⁾ G. van der Steenhoven,⁽²⁾ J. A. Tjon,⁽⁵⁾ J. Wesseling,⁽²⁾ and P. K. A. de Witt Huberts^{(1),(2)}

⁽¹⁾Department of Nuclear Physics, Rijksuniversiteit Utrecht, P.O. Box 80.000, 3508 TA Utrecht, The Netherlands

⁽²⁾Nationaal Instituut voor Kernfysica en Hoge-Energiefysica, P.O. Box 41882, 1009 DB Amsterdam, The Netherlands

⁽³⁾Institut für Kernphysik, Johannes Gutenberg-Universität, D-6500 Mainz, Germany

⁽⁴⁾Department of Physics and Astronomy, Vrije Universiteit, de Boelelaan 1081, 1081 HV Amsterdam, The Netherlands

⁽⁵⁾Institute for Theoretical Physics, Rijksuniversiteit Utrecht, P.O. Box 80.006, 3508 TA Utrecht, The Netherlands

(Received 21 October 1991)

The interference structure function f_{01} , the transverse structure function f_{11} , and the longitudinal structure function f_{00} have been determined in a ${}^2\text{H}(e,e'p)$ experiment at a four-momentum transfer $Q^2=0.21$ (GeV/c)². The f_{00} and f_{11} data are in agreement both with a nonrelativistic calculation that includes the effects of final-state interaction (FSI), meson-exchange currents, and isobar configurations, and with a relativistic calculation that only includes FSI effects. The f_{01} data demonstrate the relevance of a relativistic approach even at this low value of the momentum transfer.

PACS numbers: 25.30.Fj, 24.10.Eq, 25.10.+s, 27.10.+h

Electromagnetic studies of the deuteron have played a key role in the development of our knowledge of the deuteron wave function, nucleon-nucleon potentials, and the role of non-nucleonic degrees of freedom in nuclei. These studies mainly comprised single-arm electron-scattering experiments. Only in the last decade have these studies been augmented by coincidence experiments of the type $(e,e'p)$, which enable the determination of the nucleon momentum distribution in deuterium [1]. It was subsequently demonstrated [2] that the $(e,e'p)$ cross-section data can be fairly well described by nonrelativistic calculations using the Paris potential, provided that the influences of final-state interactions, meson-exchange currents, and isobar configurations are taken into account. In order to investigate the validity of such "exact" calculations on a deeper level it is desirable to determine the four structure functions that contribute to the (unpolarized) ${}^2\text{H}(e,e'p)$ cross section separately. Each structure function represents a different combination of nucleon current components, and thus probes a different aspect of the reaction.

A complete determination of all structure functions is experimentally very elaborate, as it involves out-of-plane measurements with high angular precision. Only one such measurement at very low momentum and energy transfer $(q,\omega)=(18\text{ MeV}, 65\text{ MeV}/c)$ has been reported so far [3]. Recently, we have determined the longitudinal structure function f_{00} and the transverse structure function f_{11} in a ${}^2\text{H}(e,e'p)$ experiment performed under quasielastic conditions [4]. Whereas the basic features of the data are reproduced by both a nonrelativistic [2] and a fully relativistic calculation [5], a 2σ deviation remains between the data and the calculations for both f_{00} and f_{11} .

Here we discuss the results of a ${}^2\text{H}(e,e'p)$ experiment, in which the interference structure function f_{01} has been determined in the quasielastic domain. As has been shown by Mosconi and Ricci [6], f_{01} is particularly sensi-

tive to relativistic effects, i.e., the treatment of the nucleon current operator in a relativistic framework. The sensitivity of f_{01} to details of the nucleon current can be surmised from its expression in terms of the three components J_0 , J_+ , and J_- of the current operator [7]: $f_{01} \sim 2\text{Re}[J_0^*(J_+ - J_-)]$. Whereas f_{00} and f_{11} depend on the square of the individual components, f_{01} depends on a product of different components. However, f_{01} is considerably smaller than f_{00} and f_{11} , implying the presence of a strong destructive interference. Consequently, f_{01} is expected to be sensitive to relatively small effects that will not show up in f_{00} and f_{11} .

The present data will be compared to two different calculations. The first is a nonrelativistic (NR) calculation due to Arenhövel [2], in which the Paris potential is used to evaluate the bound-state and continuum wave functions. The nucleon current is described using the free current operator with Sachs nucleon form factors. The calculation includes final-state-interaction (FSI) effects, meson-exchange currents (MEC), and isobar configurations (IC). The second is a fully relativistic (R) approach due to Hummel and Tjon [5], in which the strong-interaction and electromagnetic aspects of the reaction are consistently treated. A one-boson-exchange potential involving π , ρ , σ , ω , η , and δ mesons is used to describe the interaction. Furthermore, an on-shell relativistic current operator is used, with Dirac and Pauli form factors parametrized according to Höhler *et al.* [8].

The experiment was set up in such a way that simultaneously the transverse structure function f_{11} and a linear combination of f_{00} and f_{-11} could be determined. The procedure used to separate the structure functions follows from the one-photon-exchange expression of the $(e,e'p)$ cross section [9],

$$\frac{d^5\sigma}{d\omega^{\text{lab}} d\Omega_e^{\text{lab}} d\Omega_{np}^{\text{c.m.}}} = C(\rho_{00}f_{00} + \rho_{11}f_{11} + \rho_{01}f_{01}\cos\phi_{np}^{\text{c.m.}} + \rho_{-11}f_{-11}\cos 2\phi_{np}^{\text{c.m.}}). \quad (1)$$

The out-of-plane angle $\phi_{np}^{c.m.}$ represents the angle between the electron-scattering plane and the plane defined by the momentum transfer and the momentum of the outgoing proton. The kinematical quantities ρ_{ij} and C are given in Ref. [9].

The separation of f_{01} was carried out by performing measurements at $\phi_{np}^{c.m.}=0$ and $\phi_{np}^{c.m.}=\pi$, i.e., in-plane measurements forward and backward of the momentum transfer direction. As the four-momentum transfer Q is kept constant, C and ρ_{ij} are also constant for these two measurements. The difference between the two cross sections yields f_{01} . By also performing a measurement at a backward electron angle, at $\phi_{np}^{c.m.}=\pi$, and at the same value of Q , f_{11} and $f_{00} - (q^2/2Q^2)f_{-11}$ are determined. These structure functions are obtained by adding $C\rho_{01}f_{01}$ to the two cross sections measured at $\phi_{np}^{c.m.}=\pi$, and subsequently applying a Rosenbluth separation. This separation technique has been carried out at $Q^2=0.21$ (GeV/c)². A missing-momentum (p_m) range from 50 to 180 MeV/c was covered.

The measurements made use of the same experimental apparatus as has been described in Ref. [4], i.e., the NIKHEF-K two-spectrometer setup [10] in conjunction with a thin waterfall target [11] containing heavy water ²H₂O. Proton knockout from ²H and ¹⁶O was distinguished by means of cuts in the missing-energy spectrum. The large separation-energy difference between ²H and ¹⁶O and the good missing-energy resolution (≤ 500 keV) enabled an easy separation, except for the p_m range from 140 to 155 MeV/c. In this range the two peaks overlapped due to a cancellation between the separation-energy difference and the recoil-energy difference. A detailed discussion of the normalization and calibration procedures is given in Refs. [4,12].

In Table I some kinematical parameters corresponding to the central settings of the spectrometers are given. All data have been obtained at a constant momentum and energy-transfer value, centered at $(q,\omega)=(463$ MeV/c, 95.4 MeV). Therefore, the central relative neutron-proton energy in the center-of-mass is also constant, $E_{np}^{c.m.}=38.1$ MeV.

Three settings are needed for the separation procedure described above. The corresponding kinematical settings, each centered at roughly the same p_m value, are listed in Table I. However, for $p_m \approx 36$ MeV/c only two settings are listed, because these data have actually been taken in parallel kinematics, i.e., the outgoing proton momentum \mathbf{p}' is parallel to \mathbf{q} . Consequently, in this case the interference structure functions vanish, and only the longitudinal and transverse structure functions can be determined.

The calibrated deuterium target thicknesses are also given in Table I. The statistical precision of the target thickness measurement was better than 1%, while the systematic uncertainty amounts to 3%.

In addition to giving the structure functions themselves, we will also represent the data by two derived

TABLE I. Kinematics and target thicknesses of the present experiment. E_0 is the incoming electron energy, θ_e' the electron-scattering angle, θ_p' the proton emission angle, and p_m the missing momentum. The angle between \mathbf{p}' and \mathbf{q} is denoted by γ . The measured deuterium target thickness t is listed in the last column.

E_0 (MeV)	θ_e' (deg)	θ_p' (deg)	p_m (MeV/c)	γ (deg)	t (mg/cm ²)
510.5	58.92	-50.20	36.0	0.0	5.5
510.5	58.92	-28.37	175.4	-21.4	5.5
510.5	58.92	-71.04	170.0	20.9	5.8
510.5	58.92	-34.69	129.9	-15.5	5.5
510.5	58.92	-65.71	129.9	15.5	5.8
510.5	58.92	-38.68	99.9	-11.5	5.6
510.5	58.92	-61.37	97.4	11.1	6.0
510.5	58.92	-42.82	69.9	-7.4	5.9
510.5	58.92	-56.58	63.6	6.3	6.1
304.3	127.66	-32.42	99.5	11.5	6.1
304.3	127.66	-36.47	129.8	15.5	5.2
301.1	131.27	-40.32	170.2	20.8	6.2
354.2	96.73	-33.76	35.8	0.0	6.1
354.2	96.73	-41.14	69.8	7.4	6.0

quantities, the ratio \mathcal{R}_G and the asymmetry A_ϕ . Both quantities serve the purpose of bringing out some of the features of the data more clearly, while not being dependent on the normalization of the experiment. The ratio \mathcal{R}_G is defined as (with m the proton mass)

$$\mathcal{R}_G \equiv \left[\frac{2m^2}{Q^2} \frac{f_{11}}{f_{00} - (q^2/2Q^2)f_{-11}} \right]^{1/2}. \quad (2)$$

In our kinematics $(q^2/2Q^2)f_{-11}$ is estimated to be less than 3% of f_{00} . Hence, the quantity \mathcal{R}_G closely resembles the ratio R_G used in Ref. [4] as a measure of the validity of the impulse approximation with only little sensitivity to the nuclear wave function chosen.

Whereas \mathcal{R}_G is sensitive to the ratio of transverse and longitudinal components of the reaction, the asymmetry A_ϕ (see Ref. [13]) is sensitive to the longitudinal-transverse interference:

$$A_\phi \equiv \frac{\rho_{01}f_{01}}{\rho_{00}f_{00} + \rho_{11}f_{11} + \rho_{-11}f_{-11}}. \quad (3)$$

Note that A_ϕ can be obtained from the data by evaluating the cross-section asymmetry left and right of \mathbf{q} : $A_\phi = [\sigma(\phi=0) - \sigma(\phi=\pi)] / [\sigma(\phi=0) + \sigma(\phi=\pi)]$.

Before presenting the data the systematical error in the separated structure functions is considered. The uncertainties in the structure functions are generally larger than in the cross sections, mainly due to the strong angular and energy dependence of the cross sections (see, e.g., Ref. [14]). Whereas the uncertainties due to the solid angles and target thickness lead to an equally large uncertainty in the separated structure functions, the uncer-

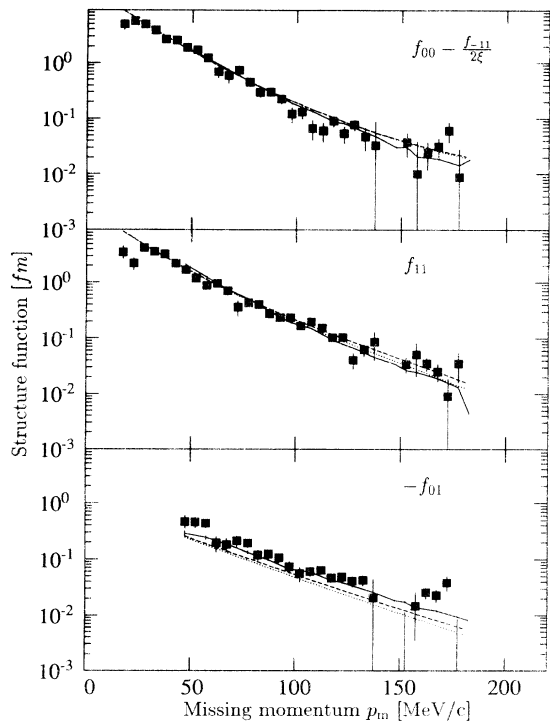


FIG. 1. Separated structure functions as a function of the missing momentum p_m . The solid curves represent the relativistic calculation of Hummel and Tjon [5] including FSI effects. The calculations of Arenhövel [2] are represented by the dashed curves (including MEC, IC, and FSI effects), and the dotted curves (FSI only). All calculations have been corrected for finite-acceptance effects [12]. Only statistical errors are shown. (Note that $\xi = Q^2/q^2$.)

tainties due to the spectrometer angles and the beam energy are different for each of the three cross sections (and correlated). Hence, these contributions have to be added, which results in relatively large systematical errors in the separated structure functions. This effect is particularly large for f_{01} because an uncertainty in the direction of \mathbf{q} (or \mathbf{p}') has an opposite effect on the cross sections at $\phi_{np}^{c.m.} = 0$ and π , respectively. Although the absolute angular position of the spectrometers at NIKHEF-K is known to better than 1 mrad, the corresponding systematical uncertainty in f_{01} is sizable: It ranges from 59% at low p_m to 27% at high p_m . The systematical uncertainty in f_{00} and f_{11} is typically 6%.

The experimental results for the structure functions $f_{00} - (q^2/2Q^2)f_{-11}$, f_{11} , and f_{01} are displayed in Fig. 1 together with the results of the theoretical calculations. The solid curves represent the relativistic (R) calculation of Hummel and Tjon [5] including FSI effects. The non-relativistic (NR) calculations of Arenhövel [2,9] are represented by the dashed (including MEC, IC, and FSI) and dotted curves (including FSI). All calculations have been corrected for finite-acceptance effects of the spectrometer pair [12]. For the f_{00} and f_{11} structure func-

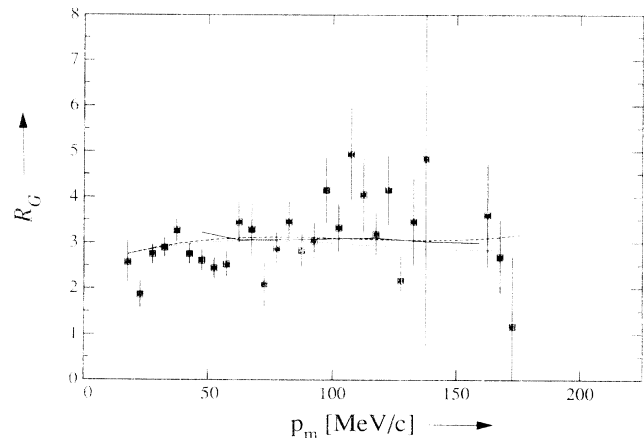


FIG. 2. The ratio \mathcal{R}_G as a function of the missing momentum. The meaning of the curves is the same as in Fig. 1. Only statistical errors are shown. The systematic uncertainty ranges from 3% to 6%.

tions the two calculations yield very similar results, and are both in fairly good agreement with the data. However, a deviation exists between the NR calculation and the f_{01} data. The R calculation is closer in this case.

In Fig. 2 the quantity \mathcal{R}_G is shown as a function of p_m . It is concluded that both calculations are in agreement with the measured transverse-longitudinal ratio. This result confirms the findings of Ref. [4], where it was shown that the quantity R_G (measured as a function of Q^2) is also well described by R and NR calculations. Since \mathcal{R}_G is a relative quantity (i.e., only ratios of cross sections are involved), the systematic errors are small (about 4%). The average ratio of the data and the calculations amounts to $0.94 \pm 0.03 \pm 0.04$ for the NR approach and $0.91 \pm 0.04 \pm 0.04$ for the R calculation.

The measured values of the asymmetry A_ϕ are compared to the calculations in Fig. 3. A substantial deviation between the NR calculations and the data is observed. A better description is given by the R calculation. In view of the systematic uncertainty on A_ϕ , which amounts to ± 0.05 on an absolute scale, the remaining deviation between the data and the R calculation is not significant. The average ratio of the A_ϕ data and the NR and R calculations is $1.87 \pm 0.08 \pm 0.47$ and $1.30 \pm 0.06 \pm 0.32$, respectively.

The MEC and IC contributions in the A_ϕ calculations of Arenhövel amount to 4% on average. Assuming that the MEC and IC effects are of similar size for the R calculations, which only include FSI effects, neither MEC nor IC contributions are likely to affect our conclusions. Moreover, in the considered kinematic region the results do not significantly depend on the choice of the interaction model. Taking wave functions constructed from the one-boson-exchange model together with the NR current operator essentially yields the same results as found using the Paris potential.

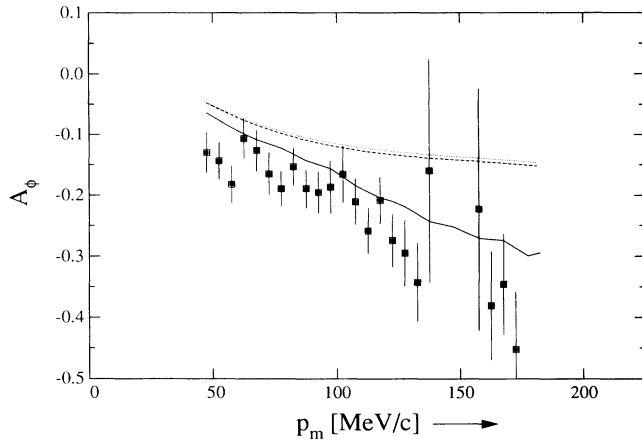


FIG. 3. The asymmetry A_ϕ as a function of the missing momentum. The meaning of the curves is the same as in Fig. 1. Only statistical errors are shown. The *absolute* systematic uncertainty is 0.05.

Finally, we turn our attention to the interpretation of the observed preference for the R calculations, although it should be added that the systematic uncertainty in both f_{01} and A_ϕ does not allow us to completely discard the NR calculation. As was pointed out previously f_{01} is particularly sensitive to the nucleon current operator employed. In the NR calculation the current operator results from truncating a q/M expansion at the first term, thus neglecting higher-order contributions. Mosconi and Ricci [6] have shown that the relativistic corrections to the nonrelativistic nucleon current result in a larger absolute value of f_{01} in our kinematic domain. Another important ingredient of the current operator concerns the choice of the nucleon form factors. Explicit NR calculations using Dirac and Pauli form factors rather than Sachs form factors also lead to larger absolute values of f_{01} , but at the same time the agreement for f_{00} is lost. We conclude that the present data cannot be described by the commonly used NR form of the current operator. On the other hand, the fully relativistic on-shell form of the nucleon current and the relativistic treatment of the wave function leads to a satisfactory description of all three measured structure functions. These results demonstrate the relevance of the experimental determination of individual structure functions.

We have presented results of a ${}^2\text{H}(e,e'p)$ experiment in quasielastic kinematics, aimed at separating more than two structure functions. Whereas the ratio of transverse and longitudinal structure functions is well described by existing calculations, the measured longitudinal-transverse interference structure function indicates the need for a relativistic approach. The origin of the difference between the f_{01} data and the nonrelativistic calculation is likely to be found in the usage of a truncated current operator with Sachs nucleon form factors. Future experiments of this type are needed to confirm and elaborate our observations. For an unambiguous interpretation of these experiments it is crucial to reduce the systematic uncertainty in f_{01} to less than 5%.

This work is part of the research program of the National Institute for Nuclear Physics and High-Energy Physics (NIKHEF-K), made possible by financial support from the Foundation for Fundamental Research on Matter (FOM) and the Netherlands' Organization for Advancement of Pure Research (NWO).

-
- [1] M. Bernheim *et al.*, Nucl. Phys. **A365**, 349 (1981).
 - [2] H. Arenhövel, Nucl. Phys. **A384**, 287 (1982).
 - [3] T. Tamae *et al.*, Phys. Rev. Lett. **59**, 2919 (1987).
 - [4] M. van der Schaar *et al.*, Phys. Rev. Lett. **66**, 2855 (1991).
 - [5] E. Hummel and J. A. Tjon, Phys. Rev. Lett. **63**, 1788 (1989); Phys. Rev. C **42**, 423 (1990).
 - [6] B. Mosconi and P. Ricci, Nucl. Phys. **A517**, 483 (1990).
 - [7] See, for instance, A. S. Raskin and T. W. Donnelly, Ann. Phys. (N.Y.) **191**, 78 (1989).
 - [8] G. Höhler *et al.*, Nucl. Phys. **B114**, 505 (1976).
 - [9] W. Fabian and H. Arenhövel, Nucl. Phys. **A314**, 253 (1979).
 - [10] C. de Vries *et al.*, Nucl. Instrum. Methods Phys. Res. **249**, 337 (1984).
 - [11] N. Voegler and J. Friedrich, Nucl. Instrum. Methods Phys. Res. **198**, 293 (1982).
 - [12] M. van der Schaar, Ph.D. thesis, Rijksuniversiteit Utrecht, 1991 (unpublished).
 - [13] H. Arenhövel, W. Leidemann, and E. L. Tomusiak, Z. Phys. A **331**, 123 (1988); **334**, 363(E) (1989).
 - [14] R. W. Lourie, in *Report of the 1987 Summer Study Group* (CEBAF, Newport News, Virginia, 1988), p. 332.